

Heterogeneous reaction of SO₂ with soot: The roles of relative humidity and surface composition of soot in surface sulfate formation



Yan Zhao ^{a, c}, Yongchun Liu ^{a, b, c, *}, Jinzhu Ma ^{a, b, c}, Qingxin Ma ^{a, b, c}, Hong He ^{a, b, c, **}

^a State Key Joint Laboratory of Environment Simulation and Pollution Control, Research Center for Eco-Environmental Sciences, Chinese Academy of Sciences, Beijing 100085, China

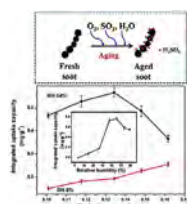
^b Center for Excellence in Regional Atmospheric Environment, Institute of Urban Environment, Chinese Academy of Sciences, Xiamen 361021, China

^c University of Chinese Academy of Sciences, Beijing 100049, China

HIGHLIGHTS

- Water promotes sulfate formation at RH in the range of 6%–70%, while exceeded water inhibits sulfate formation at RH higher than 80%.
- Soot surface composition plays important roles in SO₂ uptake and sulfate formation.
- Soot with a suitable amount of aromatic C–H and C=O groups exhibits the highest reactivity at 54% RH.

GRAPHICAL ABSTRACT



ARTICLE INFO

Article history:

Received 11 August 2016

Received in revised form

22 December 2016

Accepted 2 January 2017

Available online 3 January 2017

Keywords:

Soot

SO₂

Relative humidity

Surface composition

Sulfate formation

ABSTRACT

The conversion of SO₂ to sulfates on the surface of soot is still poorly understood. Soot samples with different fractions of unsaturated hydrocarbons and oxygen-containing groups were prepared by combusting n-hexane under well-controlled conditions. The heterogeneous reaction of SO₂ with soot was investigated using in situ attenuated total internal reflection infrared (ATR-IR) spectroscopy, ion chromatography (IC) and a flow tube reactor at the ambient pressure and relative humidity (RH). Water promoted SO₂ adsorption and sulfate formation at the RH range from 6% to 70%, while exceeded water condensed on soot was unfavorable for sulfate formation due to inhibition of SO₂ adsorption when RH was higher than 80%. The surface composition of soot, which was governed by combustion conditions, also played an important role in the heterogeneous reaction of SO₂ with soot. This effect was found to greatly depend on RH. At low RH of 6%, soot with the highest fuel/oxygen ratio of 0.162 exhibited a maximum uptake capacity for SO₂ because it contained a large amount of aromatic C–H groups, which acted as active sites for SO₂ adsorption. At RH of 54%, soot produced with a fuel/oxygen ratio of 0.134 showed the highest reactivity toward SO₂ because it contained appropriate amounts of aromatic C–H groups and oxygen-containing groups, subsequently leading to the optimal surface concentrations of both SO₂ and water. These results suggest that variation in the surface composition of soot from different sources and/or resulting from chemical aging in the atmosphere likely affects the conversion of SO₂ to sulfates.

© 2017 Elsevier Ltd. All rights reserved.

* Corresponding author. State Key Joint Laboratory of Environment Simulation and Pollution Control, Research Center for Eco-Environmental Sciences, Chinese Academy of Sciences, Beijing 100085, China.

** Corresponding author. State Key Joint Laboratory of Environment Simulation and Pollution Control, Research Center for Eco-Environmental Sciences, Chinese Academy of Sciences, Beijing 100085, China.

E-mail addresses: ycliu@rcees.ac.cn (Y. Liu), honghe@rcees.ac.cn (H. He).

1. Introduction

Soot, released from incomplete combustion of fossil fuels and biomass, consists primarily of elemental carbon (EC) and numerous organic carbon (OC) compounds (Han et al., 2012b; Jacobson, 2001; Seinfeld and Pandis, 1998). Soot particles are ubiquitous in the atmosphere, with an average emission inventory of 8–24 Tg of carbon per year (Bond, 2004; Penner et al., 1993). In the North China Plain, EC usually contributes 2%–4% to the mass concentration of PM₁₀ (Zhang et al., 2015b), although the primary organic aerosol mass fraction is found to decrease considerably during the pollution development periods (Guo et al., 2014). It has been widely recognized that soot particles in the atmosphere have an important impact on regional climate change and air quality (Ackerman, 2000; Chameides and Bergin, 2002; Peng et al., 2016; Wang et al., 2013). For example, soot particles can significantly influence the earth's radiation budget both by directly absorbing solar radiation and by indirectly scattering solar radiation as cloud condensation nuclei (CCN) (Ackerman, 2000; Chameides and Bergin, 2002). Soot may also induce adverse health effects, such as respiratory and cardiovascular diseases (Sydbom et al., 2001). In addition, when emitted into the atmosphere, soot particles undergo several aging processes, such as adsorption or condensation of gaseous species (Khalizov et al., 2009a, 2009b; Pagels et al., 2009; Peng et al., 2016; Saathoff et al., 2003; Zhang and Zhang, 2005; Zhang et al., 2008), coagulation with preexisting aerosols and heterogeneous oxidation (Han et al., 2013a, 2013b, 2012b; Lelièvre et al., 2004; Liu et al., 2010). These aging processes significantly affect soot properties, such as morphology, hygroscopic and optical properties, further influencing the climatic and health effects of soot.

In developing countries, such as China, SO₂ is still a major air pollutant, sometimes with several tens of ppbv ambient concentration (He et al., 2014; Lin et al., 2011). SO₂ can be converted to sulfates via the gas-phase oxidation, heterogeneous reactions in the aqueous phase of clouds and fog, and on transition metals (Zhang et al., 2015a). Recently, Wang et al. (2016) observed that NO₂ can efficiently promote SO₂ oxidation in aqueous media including both pure water droplets and liquid aerosols containing inorganic or organic salts formed at high relative humidity. In particular, this oxidation process is favored by the neutralization with NH₃. These reaction processes may play important roles in particulate sulfate formation during heavy haze days in China (He et al., 2014; Wang et al., 2016). For example, during the haze episode in January 2013, it was observed that the concentration of sulfates increased abruptly by 70–130 μg m⁻³ within a period of several hours in Beijing (Zheng et al., 2015a). Zheng et al. have evaluated the role of heterogeneous reactions of SO₂ in this abrupt increase during heavy haze episode. After the heterogeneous reactions of SO₂ on mineral dust were parameterized into the CMAQ model, the performance of the revised model was significantly improved for sulfate simulation (Zheng et al., 2015a). However, the highest mass concentration of sulfates was still underestimated in this work. This might be partially related to the lack of information on heterogeneous reaction of SO₂ on soot and the catalytic formation of sulfates by Fe and Mn, as pointed out by Zheng et al. (2015a). On the other hand, it has been frequently observed that soot particles are internally mixed with sulfates in the polluted urban environment and in the marine troposphere (BUseck and Pósfai, 1999; Pósfai et al., 1999; Ueda et al., 2015; Zhang et al., 2014), which greatly affects the climatic and health effects of soot. The heterogeneous reaction of SO₂ with soot has been proposed as a potentially important source of internally mixed soot and sulfates (BUseck and

Pósfai, 1999; Mészáros and Mészáros, 1989). Therefore, chemical reactions of SO₂ on soot should be paid more attention. Novakov et al. (1974) first found that propane soot could catalyze the oxidation of SO₂ to form sulfates in the presence of O₂ and water. Smith and Chughtai (1995) and Smith et al. (1989) confirmed soluble sulfate formation under similar conditions, and also observed insoluble S-O species formed under simulated solar radiation. However, it was suggested that SO₂ catalytic oxidation on the surface of soot was unimportant for atmospheric sulfate formation (Baldwin, 1982; Britton and Clarke, 1980) because the formed sulfur-containing species poisoned the soot catalyst, so that soot was unable to catalytically oxidize SO₂ to sulfates over time (Baldwin, 1982; Smith et al., 1989). Therefore, it is necessary to further investigate the reaction mechanism of SO₂ on soot to narrow the gap between modelling studies and field measurements on particulate sulfates.

Previous studies focused on the removal of SO₂ by carbonaceous materials showed that SO₂ adsorption by activated carbon increased when activated carbon was treated with concentrated nitric acid (Lisovskii et al., 1997a). However, other works indicated that the SO₂ adsorption capacity of activated carbon was inversely proportional to the amount of oxygen on the surface (Lizzio and DeBarr, 1996, 1997). Furthermore, some studies found that a pre-heating treatment of activated carbon below 1100 °C enhanced the adsorption of SO₂ because reactive sites were created accompanied with the removal of oxygen-containing functional groups (Daley et al., 1997; DeBarr et al., 1997; Li et al., 2001; Ling et al., 1999; Lisovskii et al., 1997b; Mochida et al., 1997). Meanwhile, some other studies suggested that π electrons of carbon may participate in the reaction between soot and SO₂ (Guo et al., 2013; Sun et al., 2013; Zawadzki, 1987a). In addition, surface basic groups with pyronic or pyronic-like structure were found to greatly enhance the adsorption of SO₂ on activated carbon (Davini, 1990). These previous studies suggested that chemical composition or structure played important roles in SO₂ adsorption or oxidation. Han et al. have found that the surface composition or structure of soot greatly depended on combustion conditions (Han et al., 2012a), and also observed a linear relationship between NO₂ uptake or HONO yield and the content of reduced organic carbon in soot prepared under different combustion conditions (Han et al., 2013b). However, it is as yet unknown how the surface composition of soot resulting from different combustion conditions governs the chemical oxidation of SO₂.

In the present study, soot samples were generated through combusting n-hexane under well-controlled combustion conditions. The heterogeneous reaction of SO₂ with soot was investigated using in situ attenuated total internal reflection infrared (in situ ATR-IR) spectroscopy, ion chromatography (IC) and a flow tube reactor coupled to a SO₂ analyzer at ambient pressure. The roles of relative humidity (RH) and the surface composition of soot in sulfate formation were examined in detail. These results will increase the understanding of the heterogeneous oxidation of SO₂ with soot and help to assess the possible source of internally mixed soot and sulfates in the atmosphere.

2. Experimental section

2.1. Soot production

Soot particles were obtained by burning n-hexane (AR, Sino-pharm Chemical Reagent Co., Ltd) in a co-flow system as described in several previous papers (Han et al., 2012a, 2012b, 2013a, 2013b,

Zhao et al., 2016). Soot was collected on top of a diffusion flame maintained by an airflow, which was controlled by mass flow meters to regulate the fuel/oxygen ratio. The fuel was afforded by a cotton wick extending into the liquid fuel reservoir. The airflow, a mixture of high purity O₂ and N₂, had a range of O₂ content from 29.0% to 46.5%. The combustion conditions were expressed as the molar ratio of the consumed fuel (measured by the mass of consumed n-hexane) to the introduced oxygen (obtained from the entrained airflow volume) during the combustion process. The fuel/oxygen ratio was in the range of 0.101–0.162. Soot particles produced from the diffusion flame were directly deposited on the ZnSe crystal of the ATR-IR cell, on a quartz plate and on the inner walls of a quartz tube for ATR-IR studies, ion chromatography (IC) analyses and the flow tube reactor experiments, respectively. All soot samples were collected at the exit of the burner and about 4 cm over the flame as described by Han et al. (2012b, 2013b). It should be pointed out that these cold crystal collection substrates can also lead to incomplete combustion and thus soot formation when it contacts with the diffusion flame and that soot particles produced by this method should be different from that collected generally from the flame by filter method. However, the same collection height over the flame and the similar collection substrates make sure that the incomplete combustion and thus soot formation caused by cold collection substrates almost be similar under different combustion conditions. Thus, the variations in reactivities of different soot samples toward SO₂ with soot can correctively reflect the influence of RH and surface composition of soot.

2.2. ATR-IR studies

The ATR-IR spectra were recorded using a NEXUS 6700 spectrometer (Thermo Nicolet Instrument Corp.) The Fourier transform infrared (FT-IR) spectrometer was equipped with a high sensitivity mercury cadmium telluride (MCT) detector cooled by liquid N₂. Soot particles produced from the diffusion flame were directly deposited on the ZnSe crystal of the ATR-IR cell. Compared to the mass of the ATR-IR cell, the amount of soot deposited on the ZnSe crystal was so small that we could not measure it due to the limitations of the measurement technique. The ATR-IR cell was sealed with quartz glass and purged with 100 mL min⁻¹ high purity N₂ at 298 K until the infrared spectrum showed no obvious change (about 1 h). Then, SO₂ (5 ppmv) balanced with 100 mL min⁻¹ zero air with a certain RH was introduced into the ATR-IR cell. The unreacted soot surface was taken as the reference background spectrum (100 scans, 4 cm⁻¹ resolution). The RH was recorded by a RH sensor (HMP110, HUMICAP) and controlled by changing the ratio of dry and humid zero air. The experiments were performed at 298 K at ambient pressure. The reaction of SO₂ with soot reached saturation after 540 min.

Sulfates formed on the surface of soot in ATR-IR experiments were quantified through liquid-phase calibrations with the assumption that there was little difference between the vibrational modes of sulfates in the liquid phase and those in the adsorbed phase according to a previous study (Mudunkotuwa et al., 2014). A linear calibration curve was obtained utilizing a series of aqueous solutions with known concentrations of sulfuric acid against the IR peak area of sulfate in the range of 1372–1062 cm⁻¹ (Fig. S1). Then, the amounts of sulfates formed on the soot particles under different reaction conditions were determined with this linear calibration curve. Based on this information, further quantitative analysis of sulfate formation on the surface of soot was conducted.

2.3. IC analyses

For IC measurement, about 20 mg of soot particles were spread in a quartz tube. The soot particles were subjected to a flow of SO₂ and zero air with controlled RH to start the reaction as described in the ATR-IR studies. The reaction time was also 540 min. Then, the reacted soot particles were extracted by ultrasonication with ultrapure water (specific resistance ≥ 18.2 M Ω cm) for 30 min. Sulfite oxidation in the leaching solution was suppressed by using 1% formaldehyde as a preservative as reported in the literature (Kong et al., 2014; Ullerstam et al., 2002). Then, the extract was filtered through a 0.22 μ m PTFE membrane filter. The obtained solution was analyzed using a Wayee IC-6200 ion chromatography system equipped with a SI-524E anionic analytical column. An eluent of 3.5 mM Na₂CO₃ was used at a flow rate of 0.8 mL min⁻¹.

2.4. Flow tube reactor

The uptake experiments were performed in a 34 cm length, 1.6 cm (i.d.) horizontal cylindrical coated-wall flow tube reactor (as shown in Fig. S2), which was described in detail previously (Han et al., 2013b, 2016; Liu et al., 2015a) and was similar to that used by Ndour et al. (2009). The experiments were maintained at 298 K by circulating water bath through the outer jacket of the flow tube reactor. Zero air was used as the carrier gas, and the total flow rate introduced in the flow tube reactor was 770 mL min⁻¹, ensuring a laminar regime. SO₂ was introduced into the flow tube through a movable injector with 0.3 cm radius. The SO₂ concentration was (205 \pm 5) ppbv and the experiments were performed at ambient pressure. The SO₂ concentrations were measured using a chemiluminescence analyzer (THERMO 43i) during the heterogeneous reaction of SO₂ with soot. RH was also adjusted by varying the ratio of dry zero air to wet zero air and measured by a RH sensor (HMP110, HUMICAP). It has been confirmed in control experiments that the adsorption of reactant gases on the quartz tube is negligible. The integral uptake capacity of SO₂ on unit soot sample mass was calculated with 1 min time resolution according to a method described previously (Liu et al., 2015a).

3. Results and discussion

3.1. Formation of surface sulfates

First, the heterogeneous reaction of SO₂ with soot prepared at the fuel/oxygen ratio of 0.134 was investigated at RH of 54% balanced with zero air. The unreacted soot surface was taken as the reference background spectrum. The in situ ATR-IR spectra as a function of time are shown in Fig. 1a. Sulfuric acid and bisulfate (referred to as sulfates) were clearly observed, characterized by peaks at 1196, 1030 and 912 cm⁻¹ (Querry et al., 1974). The strong absorption peak centered at 1196 cm⁻¹ was assigned to the asymmetric stretching of H₂SO₄ and the peak at 912 cm⁻¹ was assigned to the symmetric stretching of H₂SO₄ (Querry et al., 1974). The peak at 1030 cm⁻¹ was attributed to the stretching modes of HSO₄⁻ (Querry et al., 1974). Meanwhile, a peak corresponding to sulfite or strongly adsorbed SO₂ on the surface of soot was found at 1045 cm⁻¹ (Zawadzki, 1987a, b). Peaks centered at 3470, 3380, 3425 and 1635 cm⁻¹ due to H₂O (Lu et al., 2008; Ma et al., 2010) appeared in the spectra. As the reaction proceeded, these peaks increased in intensities, which suggests that sulfuric acid and bisulfate as well as sulfite are formed and water is adsorbed and aggregated on the surface of soot in the heterogeneous reaction of SO₂ with soot. Moreover, a peak at 1580 cm⁻¹ appeared accompanied by an increase in intensity as the heterogeneous reaction proceeded. Based on previous works concerning oxygen adsorption

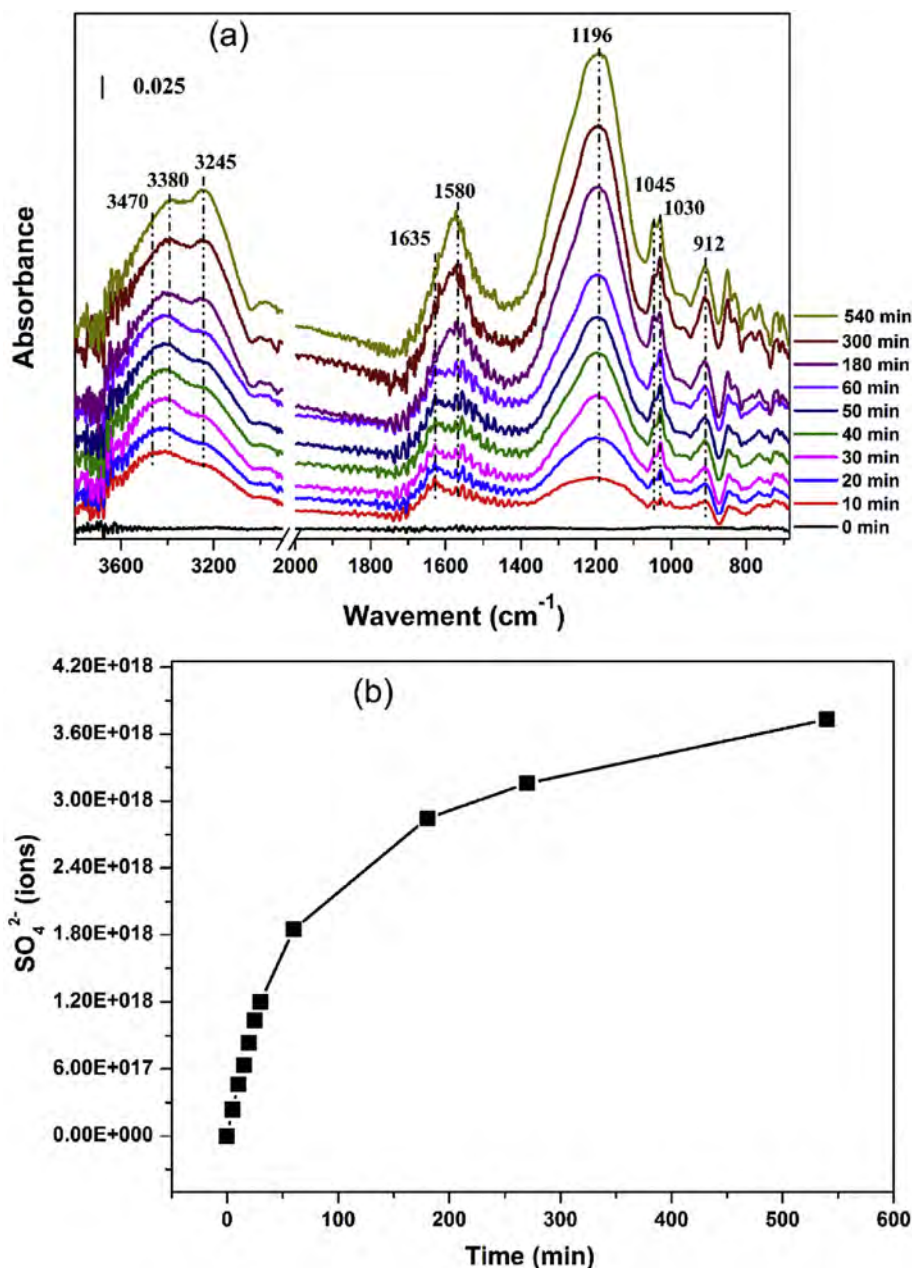


Fig. 1. (a) Dynamic changes in the ATR-IR spectra of soot as a function of time. (b) Sulfate formation on soot as a function of time during the reaction with SO₂. ATR-IR reaction conditions: total flow rate of 100 mL min⁻¹, 5 ppmv SO₂ + zero air, soot with fuel/oxygen ratio of 0.134, RH of 54%, temperature of 298 K.

on carbonaceous materials (Zawadzki, 1978, 1987b), the peak at 1580 cm⁻¹ was attributed to oxygen chemisorption on carbon. This assignment was further confirmed by the ATR-IR spectra of soot when exposed to SO₂ in the absence of O₂. As shown in Fig. S3, the peak at 1580 cm⁻¹ did not appear when soot was exposed to SO₂ and water vapor balanced with high purity N₂. In addition, there was a prominent loss of intensity for the peak at 876 cm⁻¹ due to a substituted aromatic C–H group (Cain et al., 2010; Han et al., 2012a; Kirchner et al., 2000; Smith and Chughtai, 1995) as the reaction proceeded, implying that π electrons of carbon may be consumed or disturbed, and involved in the heterogeneous reaction of SO₂ with soot in the presence of O₂ and H₂O. This phenomenon is in good agreement with results in the literature focusing on SO₂ adsorption on carbonaceous materials, in which π electrons of carbon were found to participate in the adsorption of SO₂ and O₂ on soot (Sun et al., 2013; Zawadzki, 1987a). The mechanism will be

discussed later.

Fig. 1b shows the sulfate formation as a function of reaction time through the heterogeneous reaction of SO₂ with soot. Sulfates formed on the surface of soot increased linearly in the first 30 min and after that they increased much more slowly until the end of the reaction.

3.2. Role of the relative humidity in sulfate formation

Previous studies indicated that water was essential to sulfate formation in the heterogeneous reaction of SO₂ with soot (Novakov et al., 1974; Smith et al., 1989). However, the role of water in this reaction is not fully understood. Therefore, the effect of water on the heterogeneous reaction of SO₂ with soot was investigated at ambient RH ranging from 6% to 89% using ATR-IR, IC and a flow tube reactor with soot produced at a constant fuel/oxygen ratio of 0.134.

The trends of sulfate formation were similar when the RH was below 70%, while sulfate formation slowed down more rapidly after 30 min when the RH was greater than 80% as shown in Fig. S4a.

However, the total amounts of sulfates formed at the end of the reaction after 540 min for different RH were dramatically different as shown Fig. 2a. The total amount of sulfates increased from 1.076×10^{18} ions to 3.840×10^{18} ions as RH increased from 6% to 70%, and then markedly decreased to 2.983×10^{18} ions when RH rose to 89%. Moreover, the amount of sulfates formed per unit soot mass was in the range of 0.249–0.805 mg g^{-1} based on IC analysis. The variation trend of the total amount of sulfates as a function of RH obtained from IC agreed well with that from ATR-IR. This confirms the reliability of the sulfate formation results obtained from ATR-IR.

On the basis of the results of many studies focusing on SO_2 removal by carbonaceous material at relatively low temperatures (Lisovskii et al., 1997a; Liu et al., 2003; Lizzio and DeBarr, 1997; Rubio and Izquierdo, 1998; Zhang et al., 2007), the sulfate formation rate on the surface of soot can be given by equation (1),

$$\frac{d[\text{H}_2\text{SO}_4]}{dt} = k[\text{SS}][\text{SO}_2]^a[\text{O}_2]^b[\text{H}_2\text{O}]^c \quad (1)$$

where k refers the rate constant of the reaction, a , b , and c are the reaction orders for SO_2 , O_2 and H_2O , respectively. SS refers to surface sites, including SS_1 for SO_2 and O_2 adsorption, which involves the participation of π electrons of carbon (Zawadzki, 1978, 1987a, b), and SS_2 for H_2O adsorption, which mainly occurs on the polar oxygen-containing groups on the surface of soot particles.

In the initial stage of the reaction, the amount of sulfates formed on the surface of soot was small compared to the surface active sites, thus the active sites can be considered constant. Fig. S4b shows the linear dependence of the amount of sulfates formed on reaction time within the first 25 min. The slopes of these lines represented the apparent formation rates of sulfates. Fig. 2b shows the apparent formation rate of sulfates as a function of RH in the range from 6% to 89%. The apparent formation rate of sulfates increased from $(6.334 \pm 0.085) \times 10^{15}$ ions $\cdot \text{min}^{-1}$ to $(7.582 \pm 0.045) \times 10^{17}$ ions $\cdot \text{min}^{-1}$ with RH increasing from 6% to 89%.

The reaction order of H_2O was obtained from the slope of the log-log plot of the apparent formation rate of sulfates versus the water concentration as shown in Fig. 2c. The reaction order of $\text{H}_2\text{O}(\text{g})$ was calculated as (0.756 ± 0.072) with RH in the range of 6%–89%. This value was close to the value of 0.5 obtained by Yamamoto et al. (1972). The reaction order for H_2O was lower than 1, indicating the presence of Langmuir–Hinshelwood mechanism, which was in agreement with previous results that H_2O was adsorbed on the surface of soot and reacted to form sulfuric acid in the presence of O_2 and SO_2 (Lizzio and DeBarr, 1997; Rubio and Izquierdo, 1998).

Combining the amounts of sulfates formed with the apparent formation rates of sulfates at different RH, it can be suggested that the effect of water on sulfate formation in the heterogeneous reaction of SO_2 with soot is closely related to the amount of surface water in terms of RH. At RH in the range of 6%–70%, increasing water can greatly promote sulfate formation, with an increase in the amount of sulfates formed and the apparent formation rates of sulfates. However, when RH was high than 80%, water enhanced the sulfate formation rate at the initial stage of reaction, but reduced the amount of sulfates formed at steady state. These phenomena imply that an appropriate amount of surface water can promote sulfate formation, while exceeded surface water is unfavorable to sulfate formation on the surface of soot.

As mentioned above, SO_2 and water were first adsorbed on the

surface of soot, then oxidized and hydrated to form sulfates (Lisovskii et al., 1997a; Lizzio and DeBarr, 1997; Rubio and Izquierdo, 1998; Zhang et al., 2007), it can be proposed that too much water absorbed on the surface of soot may inhibit SO_2 uptake when RH is higher. This assumption was further confirmed by the uptake of SO_2 on soot pre-saturated with water using a flow tube reactor. The results are shown in Fig. 2d. The uptake capacity of SO_2 per unit soot mass within the first 60 min increased from $(0.193 \pm 0.005) \text{ mg} \cdot \text{g}^{-1}$ to $(0.585 \pm 0.016) \text{ mg} \cdot \text{g}^{-1}$ as RH increased from 6% to 70%, and then decreased to $(0.473 \pm 0.011) \text{ mg} \cdot \text{g}^{-1}$ when RH increased to 89%, confirming the assumption that an appropriate amount of surface water can promote SO_2 adsorption and sulfate formation while exceeded water on the surface of soot is unfavorable for SO_2 adsorption. When RH was high at 80%, exceeded water were absorbed and condensed on soot. In this case, condensation of water may cause steric hindrance to SO_2 uptake on soot. A similar result was also obtained in a previous study in which a moderate H_2O content of 7% was appropriate for SO_2 removal from flue gas by activated semi-cokes, while more or less H_2O content was unfavorable to SO_2 removal (Liu et al., 2003). Furthermore, based on the results of IC and uptake experiments, the yield of sulfates was calculated as about 95%. This result was in accordance with the results of ATR-IR, indicating that SO_2 adsorbed on soot was mainly converted to sulfates, and only a small portion existed in the form of sulfite or adsorbed SO_2 .

3.3. Role of surface composition in sulfate formation

Our previous studies indicated that soot produced at different fuel/oxygen ratios showed variations in surface properties. For example, the contents of saturated and unsaturated hydrocarbons as well as partially oxidized organics condensed onto the surface of soot varied with the fuel/oxygen ratio (Han et al., 2012a, 2012b). Subsequently, it has been found that the reactivity of soot toward NO_2 varies depending on the combustion conditions for production of soot (Han et al., 2013a, 2013b). However, how the combustion conditions of soot influence the reactivity of soot toward SO_2 is still unknown. Therefore, the role of the surface composition of soot in the heterogeneous reaction of SO_2 with soot was investigated at a constant RH of 54%. The trend of sulfate formation, the total amount of sulfates and the sulfate formation rate on the surface of soot were analyzed as described above, and the results are shown in Fig. 3. The trends of sulfate formation on soot produced at different fuel/oxygen ratios as a function of time were similar, presenting an initial linear increase, followed by rapid and finally slow increase as shown in Fig. S5a. The total amounts of sulfates formed on the surface of soot increased from 1.908×10^{18} ions to 3.978×10^{18} ions as the fuel/oxygen ratio rose from 0.100 to 0.134, then decreased to 1.328×10^{18} ions when the fuel/oxygen ratio further rose to 0.162. Meanwhile, the total amounts of sulfates obtained from analysis of IC results were in good agreement with those of ATR-IR as shown in Fig. 3a, suggesting that soot produced at the fuel/oxygen ratio of 0.134 showed a maximum formation capacity for sulfates. In addition, it can be clearly observed from Fig. 3b that soot produced at the fuel/oxygen ratio of 0.134 presented the highest apparent sulfate formation rate of $(5.933 \pm 0.121) \times 10^{16}$ ions $\cdot \text{min}^{-1}$ within the first 25 min of reaction, which confirmed that soot produced at the fuel/oxygen ratio of 0.134 showed the highest reactivity toward SO_2 .

As observed in Fig. 2d, surface water was favorable for the uptake of SO_2 on soot when the amount of surface water was below the critical value obtained for the soot prepared at the fuel/oxygen ratio of 0.134 and at RH of 54%–70%. At RH of 6%, it was reasonable to propose that such a critical value of surface water did not reached even when the fuel/oxygen ratio was lower than 0.134. As observed

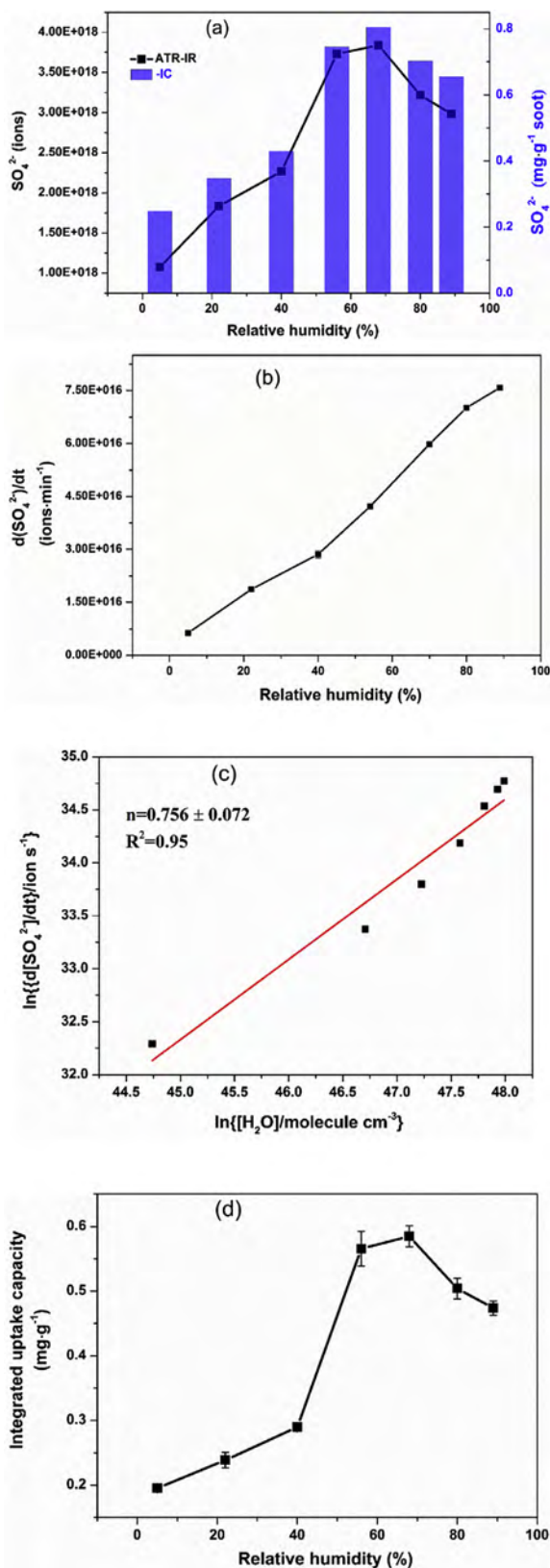


Fig. 2. (a) Amounts of sulfates formed on soot after reaction for 540 min as a function of relative humidity. (b) The apparent formation rate of sulfates on soot as a function of relative humidity within the first 25 min of reaction. (c) Log-log plot of the apparent sulfate formation rate versus $[\text{H}_2\text{O}]$. (d) Uptake capacity of SO_2 on soot saturated with water within the first 60 min as a function of relative humidity. Figs. a, b and c were obtained from ATR-IR. ATR-IR reaction conditions: total flow rate of 100 mL min^{-1} , $5 \text{ ppmv SO}_2 + \text{zero air}$, soot with fuel/oxygen ratio of 0.134, temperature of 298 K. Fig. d

in our previous work (Han et al., 2012a), soot prepared at a low fuel/oxygen ratio was more hydrophilic than the counterpart because of the higher content of C=O groups and the lower content of aromatic C–H groups as shown in Fig. S6. This implies that the SO_2 uptake capacity at RH of 6% should decrease as a function of the fuel/oxygen ratio if surface water was the sole factor determining the uptake of SO_2 . However, an opposite relationship between the SO_2 uptake capacity and the fuel/oxygen ratio in Fig. S7 was observed when RH was 6%. This implies that surface composition of soot played a key role in the heterogeneous reaction of SO_2 besides surface water.

Based on the IR spectra of the heterogeneous reaction of SO_2 with soot in this study and previous works focused on SO_2 adsorption on carbonaceous materials in the presence of O_2 and H_2O (Guo et al., 2013; Sun et al., 2013; Zawadzki, 1987a, b), it has been proposed that π electrons of carbon participate in the heterogeneous reaction of SO_2 with soot. It is well recognized that π electrons exist in the aromatic rings of carbonaceous materials. Thus, π electrons can be most probably related to the aromatic C–H groups of soot investigated in this study. Therefore, the ratio of peak areas of all aromatic C–H groups (including aromatic C–H and highly substituted aromatic C–H groups) to peak areas of all groups (consisting of carbonyl (C=O) group bound to aromatic rings and total C–H groups including aromatic C–H group, substituted aromatic C–H groups, alkyne $\equiv\text{C}$ –H group and unsaturated C–H ($=\text{CH}_2$) groups), $A_{\text{aromatic C-H}}/A_{\text{C-H+C=O}}$, can be considered to be a measurement of the amounts of reduced π electrons on soot. It has been known that $A_{\text{aromatic C-H}}/A_{\text{C-H+C=O}}$ increases with increasing fuel/oxygen ratio as shown in Fig. S6. This suggests that more reduced π electrons exist on soot produced at a higher fuel/oxygen ratio. Fig. 4 shows the uptake capacity of SO_2 versus $A_{\text{aromatic C-H}}/A_{\text{C-H+C=O}}$ corresponding to soot produced at different fuel/oxygen ratios at low RH of 6%. It was obvious that there was a good linear correlation between the uptake capacity of SO_2 and $A_{\text{aromatic C-H}}/A_{\text{C-H+C=O}}$, suggesting that reduced π electrons in aromatic C–H groups on the surface of soot were the main active sites for SO_2 uptake at low RH of 6%. It also means that the reduced π electrons dominate the heterogeneous uptake of SO_2 at low RH (6%).

Fig. 5a shows the uptake capacity of SO_2 on soot as a function of the fuel/oxygen ratio at RH of 54%. The uptake capacity of SO_2 on soot increased from $(0.456 \pm 0.011) \text{ mg}\cdot\text{g}^{-1}$ to $(0.565 \pm 0.020) \text{ mg}\cdot\text{g}^{-1}$ with increasing fuel/oxygen ratio from 0.101 to 0.134, and then decreased to $(0.366 \pm 0.015) \text{ mg}\cdot\text{g}^{-1}$ as the fuel/oxygen ratio increased to 0.162, which was the same as the trends of total amounts of sulfates formed and the sulfate formation rate as shown in Fig. 3. Compared with the uptake of SO_2 on soot at low RH of 6%, the uptake capacities of SO_2 on soot at RH of 54% were higher on soot produced at corresponding fuel/oxygen ratios. Meanwhile, the variation trend of the uptake capacities of SO_2 versus the fuel/oxygen ratios at low RH were entirely different from that at high RH. These results imply that increasing water can enhance the uptake of SO_2 on soot. Meanwhile, it can be indicated that the role of surface composition of soot governed by the fuel/oxygen ratio in the heterogeneous reaction of SO_2 with soot was greatly dependent on RH. Soot with the fuel/oxygen ratio lower than 0.134 contained more C=O groups and less aromatic C–H groups. At RH of 54%, the limited number of the reduced π electrons in aromatic C–H groups and exceeded surface water induced by more C=O groups inhibited the uptake of SO_2 on this kind of soot. Soot with the fuel/oxygen ratio higher than 0.134 contains fewer C=O groups and more

was obtained from the flow tube reactor results. Flow tube reaction conditions: total flow rate of 770 mL min^{-1} , $(205 \pm 5) \text{ ppbv SO}_2 + \text{zero air}$, soot with fuel/oxygen ratio of 0.134, temperature of 298 K.

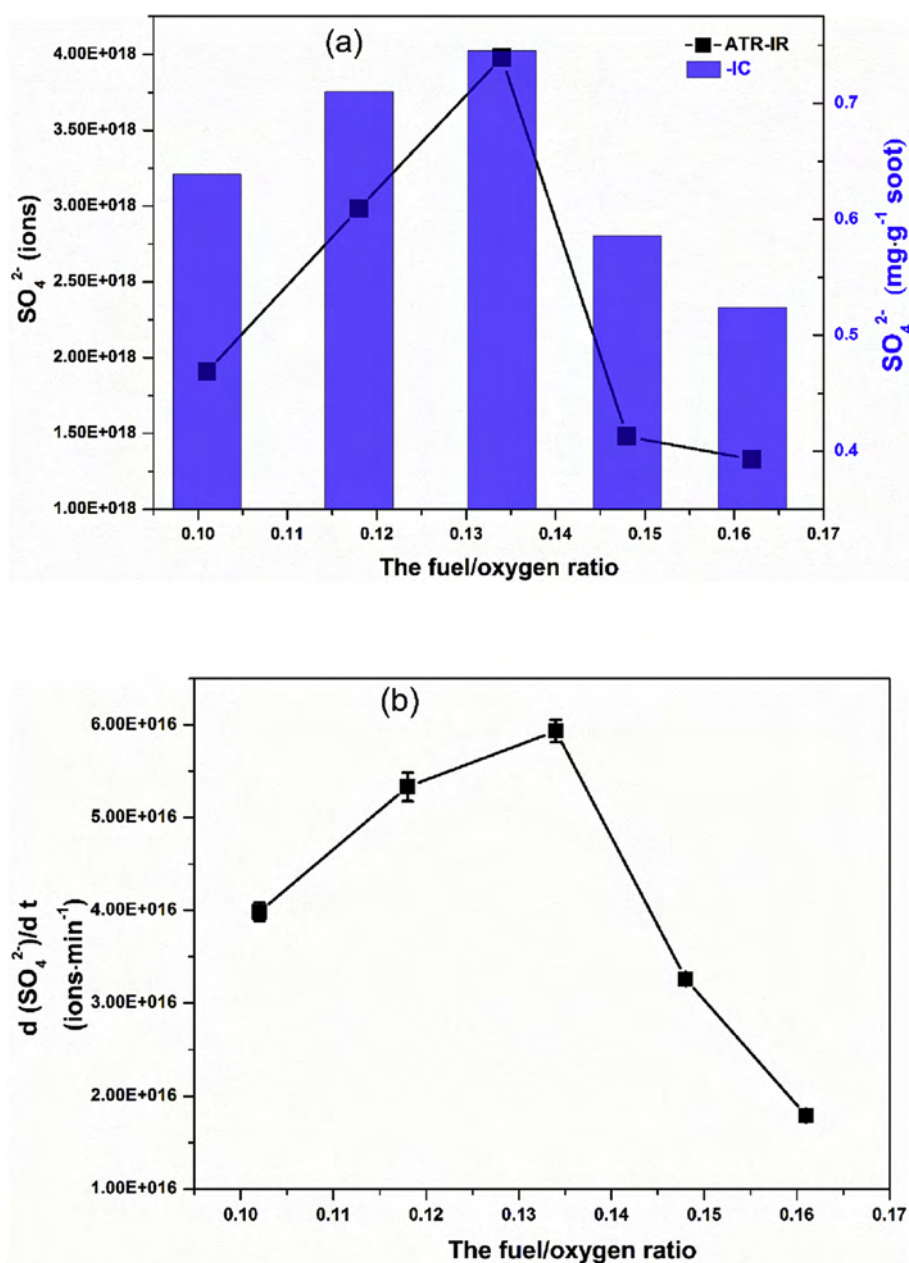


Fig. 3. (a) Amounts of sulfates formed after reaction for 540 min on soot as a function of the fuel/oxygen ratio. (b) The apparent sulfate formation rate on soot as a function of the fuel/oxygen ratio within the first 25 min of reaction. ATR-IR reaction conditions: total flow rate of 100 mL min^{-1} , 5 ppmv SO_2 + zero air, RH of 54%, temperature of 298 K.

aromatic C–H groups. In this case, although more reduced π electrons were available, insufficient surface water due to hydrophobic soot limited the uptake of SO_2 when RH was 54%. Therefore, a suitable amount of surface water and SO_2 adsorption sites (the reduced π electrons) led to the maximum SO_2 uptake capacity at RH of 54% and the fuel/oxygen ratio of 0.134 (Fig. 5d). The above results mean that the role of the reduced π electrons is dominant in the heterogenous uptake of SO_2 when surface water was very low (RH 6%), while the role of surface water becomes more important and complicated when RH was high (54%) although the reduced π electrons may still have influence on the uptake of SO_2 . Moreover, the result of SO_2 uptake on soot with the fuel/oxygen ratio lower than 0.134 at RH of 54% is consistent with that at higher RH than 80%, whereby exceeded water absorbed and condensed on soot might hinder SO_2 adsorption as discussed in Section 3.2. In

addition, it can be further inferred that exceeded water absorbed and condensed on C=O groups that were connected with aromatic rings would produce the steric hindrance effect for SO_2 uptake on soot at high RH.

Moreover, the sulfate formation and SO_2 uptake on aged soot were also investigated to confirm the roles of aromatic C–H groups and C=O groups in the reactivity of soot toward SO_2 as detailed in Supporting Information. Soot was first exposed to 2 ppmv O_3 and then exposed to SO_2 . It can be observed from Fig. 6a and Table 1 that sulfate formation and SO_2 uptake on soot produced at a higher fuel/oxygen ratio of 0.162 greatly increased after soot was aged by O_3 , suggesting an increase in the reactivity of soot toward SO_2 . For soot produced at a relatively lower fuel/oxygen ratio of 0.134, the reactivity of soot toward SO_2 significantly decreased, presenting decreases in sulfate formation and SO_2 uptake on aged soot by O_3 as

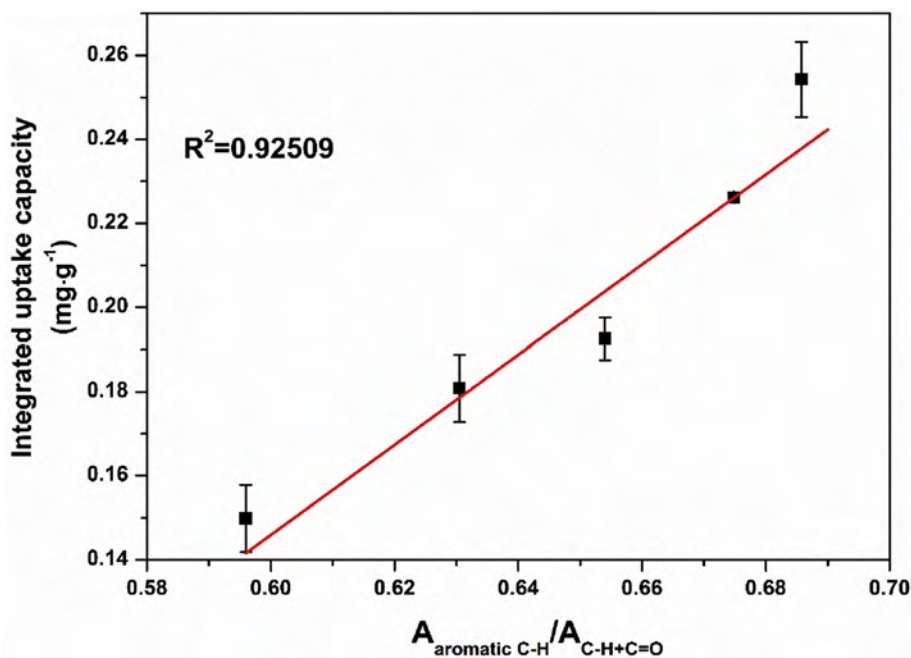


Fig. 4. Plot of uptake capacity of SO_2 versus $A_{\text{aromatic C-H}}/A_{\text{C-H+C=O}}$ on soot at low RH of 6% within the first 60 min of reaction. Flow tube reaction conditions: total flow rate of 770 mL min^{-1} , (205 ± 5) ppbv SO_2 + zero air, RH of 6%, temperature of 298 K.

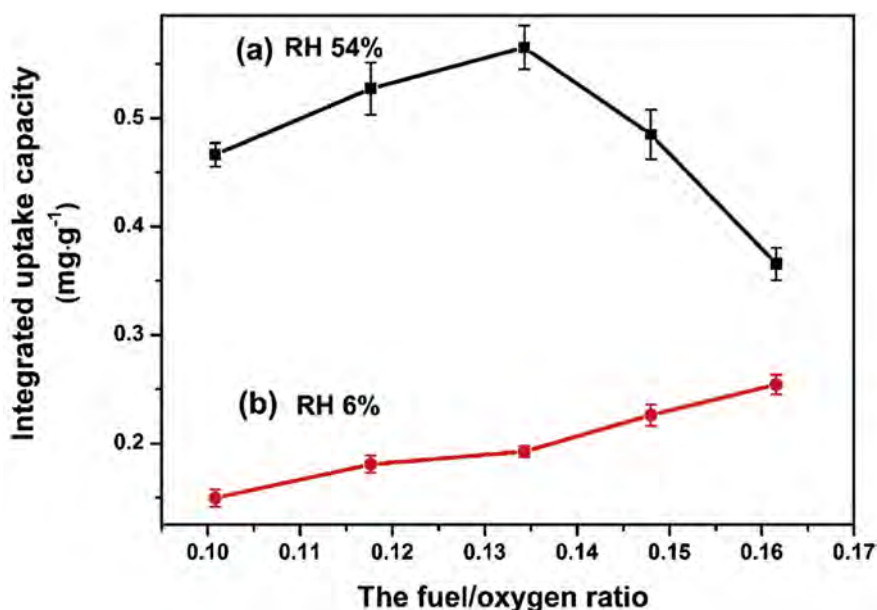


Fig. 5. Uptake capacity of SO_2 on soot pre-saturated by water as a function of the fuel/oxygen ratio within the first 60 min of reaction. (a) RH of 54%. (b) RH of 6%. Flow tube reaction conditions: total flow rate of 770 mL min^{-1} , (205 ± 5) ppbv SO_2 + zero air, temperature of 298 K.

shown in Fig. 6b and Table 1. We have known that there were a large amount of aromatic C–H groups and a small amount of C=O groups on soot produced at a higher fuel/oxygen ratio of 0.162. Soot aged by O_3 decreased the amount of aromatic C–H groups and correspondingly increased the amount of C=O groups. Thus, appropriate amounts SO_2 and H_2O could be adsorbed on soot and the reactivity of soot toward SO_2 increased. For soot produced at a lower fuel/oxygen ratio of 0.134 that contained appropriate amount of aromatic C–H groups and amount of C=O groups, ozonation consumed aromatic C–H groups and produced C=O groups. Consequently, a large amount of C=O groups existed on the surface

of soot. In this case, more H_2O could be adsorbed while less SO_2 was available on soot. This is consistent with the dependence of the uptake capacity of SO_2 on the fuel/oxygen ratio at RH of 54% (Fig. 5a). Therefore, it can be concluded that surface composition, such as aromatic C–H groups and C=O groups on the surface of soot, played key roles in the reactivity of soot toward SO_2 .

At the present time, the mechanism by which oxygen is activated for SO_2 oxidation remains largely unknown, although Hung and Hoffmann (2015) suggested that there was an efficient pathway via sulfite and sulfate radical anions on acidic microdroplets in which the direct interfacial electron transfer from HSO_3^-

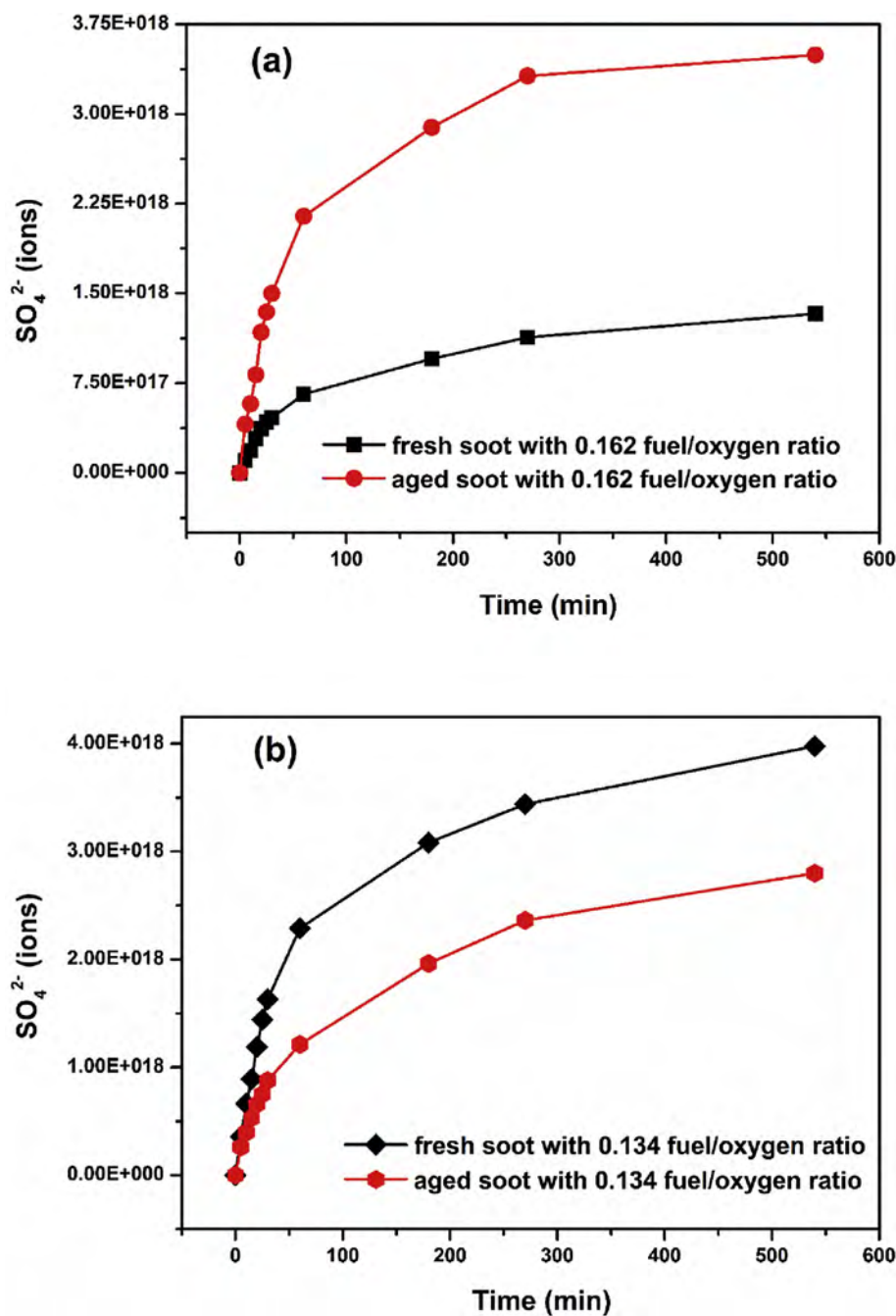


Fig. 6. Sulfate formation on fresh soot and soot oxidized by 2 ppmv O_3 as a function of time with different fuel/oxygen ratio. (a) Soot with the fuel/oxygen ratio of 0.162; (b) Soot with the fuel/oxygen ratio of 0.134. ATR-IR reaction conditions: total flow rate of 100 mL min^{-1} , $5 \text{ ppmv SO}_2 + \text{zero air}$, RH of 54%, temperature of 298 K.

Table 1

SO_2 integrated uptake capacity on fresh soot and soot oxidized by 2 ppmv O_3 . Flow tube reaction conditions: total flow rate of 770 mL min^{-1} , $(205 \pm 5) \text{ ppbv SO}_2 + \text{zero air}$, temperature of 298 K.

The fuel/oxygen ratio	SO_2 integrated uptake capacity ($\text{mg} \cdot \text{g}^{-1}$ soot)	
	Fresh soot	Aged soot by O_3
0.162	0.366 ± 0.015	0.567 ± 0.084
0.134	0.565 ± 0.020	0.343 ± 0.014

to O_2 occurred. It has been found that reactive oxygen species (ROS) can be formed on the surface of black carbon (Li et al., 2013), carbon

nanotubes (Liu et al., 2015b) and soot particles (Peebles et al., 2011) in the presence of water. The formation of ROS in this way has been considered as a mechanism leading to oxidative stress in the human respiratory tract (Gehling et al., 2014). In this work, ROS (mainly superoxide radicals) were observed in the EPR spectrum of an aqueous solution of soot (seen in Fig. S8) in the presence of O_2 . Therefore, it can be inferred that superoxide radicals were formed on the surface of soot when a certain amount of water existed in the presence of O_2 at RH of 54% in our study. The complicated influences of RH and the surface properties of soot on the oxidation activity of SO_2 might also be partially ascribed to the differences in ROS formation activity on the surface of soot particles.

4. Conclusions and implications

In this study, the roles of RH and soot surface composition in the heterogeneous reaction of SO₂ with soot were examined. Water promoted sulfate formation at ambient RH from 6% to 70%, while exceeded water adsorption and aggregation on soot was unfavorable for SO₂ adsorption and sulfate formation when RH was high than 80%. The role of soot surface composition governed by the combustion conditions in the heterogeneous reaction of SO₂ with soot was highly dependent on ambient RH. At low RH of 6%, soot with the highest fuel/oxygen ratio showed the maximum uptake capacity for SO₂ since it contained more aromatic C–H groups, which were the main active sites for SO₂ adsorption. At high RH of 54%, soot produced with the moderate fuel/oxygen ratio of 0.134 showed the highest reactivity toward SO₂. This was because there were appropriate amounts of aromatic C–H groups and C=O groups on this kind of soot sample, which induced appropriate uptake of both SO₂ and water and favored sulfate formation.

Soot represents a major constituent of atmospheric aerosols and is ubiquitous in the atmosphere produced from various combustion sources. It has been known from our previous works that more C–H species, such as aromatic hydrocarbons, exist on the surface of soot with the higher fuel/oxygen ratio, while more C=O species appear for soot with the lower fuel/oxygen ratio (Han et al., 2012a, 2012b). In dry conditions with low RH of 6%, the soot with the higher fuel/oxygen ratio shows a large uptake capacity for SO₂. At RH of 50%, larger amounts of SO₂ can be adsorbed on soot with the lower fuel/oxygen ratio, thus leading to more sulfate formation. Meanwhile, it should be noted that at high RH, such as 80%, an excess amount of water is condensed on the surface of soot, which inhibits the uptake of SO₂ on soot and decreases sulfate formation. Similarly, for soot generated at the extremely low fuel/oxygen ratio of 0.101, a large amount of C=O species existing on the surface of soot can induce exceeded water to be adsorbed on soot, leading to a decrease in the uptake of SO₂ on soot. It should be pointed out that heavy haze events usually were accompanied with high RH (>80%) in winter time in Beijing (Sun et al., 2016; Zheng et al., 2015b). Although decreasing to some extent at RH higher than 80% when compared with RH of 54%, SO₂ uptake and sulfate formation are still more rapid than those of RH below 40% usually in clean days. Therefore, it can be inferred that the heterogeneous reaction of SO₂ with soot might contribute to the rapid sulfate formation at high RH conditions during haze episodes.

Moreover, it is well known that soot will undergo aging processes via heterogeneous oxidation by O₃, O₂, OH, N₂O₅ and HNO₃ (Bertram et al., 2001; Han et al., 2012b; Lelièvre et al., 2004; McCabe and Abbatt, 2009; Monge et al., 2010; Saathoff et al., 2001) once emitted into the atmosphere. The oxidation aging will decrease surface aromatic C–H groups and increase surface oxygen-containing species to some extent. As we observed in this study, the oxidation aging increased the reactivity of soot produced at a higher fuel/oxygen while decreased the reactivity of soot with a lower fuel/oxygen ratio in the heterogeneous reaction of SO₂ with soot. Therefore, it can be concluded that the heterogeneous reaction between soot and SO₂ is significantly affected by the surface composition of soot and RH. When considering the sulfate formation resulting from this heterogeneous reaction in the atmosphere, the influences of the surface composition of soot and RH should be paid more attention. This study provides new information on the heterogeneous reactions of SO₂ with soot and helps more comprehensively assess this reaction and the corresponding environmental effects.

In addition, the heterogeneous reaction between SO₂ and soot results in a sulfate coating on the surface of soot, which might be a potentially important source for the internally mixed soot and

sulfates (BUSECK and Pósfai, 1999; Mészáros and Mészáros, 1989), and could greatly affect the climate effects of sulfates and soot aerosols (Zhang et al., 2008). Meanwhile, the heterogeneous reaction of SO₂ with soot transforms initially hydrophobic soot into hygroscopic soot. This transformation will further lead to dramatic changes in physicochemical characteristics of soot in the atmosphere. The enhanced hygroscopicity of soot will facilitate the formation of a water layer over soot, inducing a restructuring of soot aggregates. Furthermore, the water layer facilitates adsorption and reaction of other pollutants in the surrounding air.

Acknowledgments

The research was financially supported by the Strategic Priority Research Program of the Chinese Academy of Sciences (XDB05010300), National Natural Science Foundation of China (91543109) and Ministry of Science and Technology of China (2016YFC0203700). The authors thank the group of Yujing Mu for their help with the IC measurements.

Appendix A. Supplementary data

Supplementary data related to this article can be found at <http://dx.doi.org/10.1016/j.atmosenv.2017.01.005>.

References

- Ackerman, A.S., 2000. Reduction of tropical cloudiness by soot. *Science* 288, 1042–1047.
- Baldwin, A.C., 1982. Heterogeneous reactions of sulfur dioxide with carbonaceous particles. *Int. J. Chem. Kinet.* 14, 269–277.
- Bertram, A.K., Ivanov, A.V., Hunter, M., Molina, L.T., Molina, M.J., 2001. The reaction probability of OH on organic surfaces of tropospheric interest. *J. Phys. Chem. A* 105, 9415–9421.
- Bond, T.C., 2004. A technology-based global inventory of black and organic carbon emissions from combustion. *J. Geophys. Res.* 109 <http://dx.doi.org/10.1029/2003jd003697>.
- Britton, L.G., Clarke, A.G., 1980. Heterogeneous reactions of sulphur dioxide and SO₂/NO₂ mixtures with a carbon soot aerosol. *Atmos. Environ.* 14, 829–839.
- BUSECK, P.R., Pósfai, M., 1999. Airborne minerals and related aerosol particles. Effects on climate and the environment. *Proc. Natl. Acad. Sci. U. S. A.* 96, 3372–3379.
- Cain, J.P., Gassman, P.L., Wang, H., Laskin, A., 2010. Micro-FTIR study of soot chemical composition—evidence of aliphatic hydrocarbons on nascent soot surfaces. *Phys. Chem. Chem. Phys.* 12, 5206–5218.
- Chameides, W.L., Bergin, M., 2002. Soot takes center stage. *Science* 297, 2214–2215.
- Daley, M.A., Mangun, C.L., DeBarr, J.A., Riha, S., Lizzio, A.A., Donnals, G.L., Economy, J., 1997. Adsorption of SO₂ onto oxidized and heat-treated activated carbon fibers (ACFs). *Carbon* 35, 411–417.
- Davini, P., 1990. Adsorption and desorption of SO₂ on active carbon: the effect of surface basic groups. *Carbon* 28, 565–571.
- DeBarr, J.A., Lizzio, A.A., Daley, M.A., 1997. Adsorption of SO₂ on bituminous coal char and activated carbon fiber. *Energy. Fuel* 11, 267–271.
- Gehling, W., Khachatryan, L., Dellinger, B., 2014. Hydroxyl radical generation from environmentally persistent free radicals (EPFRs) in PM_{2.5}. *Environ. Sci. Technol.* 48, 4266–4272.
- Guo, S., Hu, M., Zamora, M.L., Peng, J., Shang, D., Zheng, J., Du, Z., Wu, Z., Shao, M., Zeng, L., Molina, M.J., Zhang, R., 2014. Elucidating severe urban haze formation in China. *Proc. Natl. Acad. Sci. U. S. A.* 111, 17373–17378.
- Guo, Y., Li, Y., Zhu, T., Ye, M., Wang, X., 2013. Adsorption of SO₂ and chlorobenzene on activated carbon. *Adsorption* 19, 1109–1116.
- Han, C., Liu, Y., He, H., 2013a. Heterogeneous photochemical aging of soot by NO₂ under simulated sunlight. *Atmos. Environ.* 64, 270–276.
- Han, C., Liu, Y., He, H., 2013b. Role of organic carbon in heterogeneous reaction of NO₂ with soot. *Environ. Sci. Technol.* 47, 3174–3181.
- Han, C., Liu, Y., Liu, C., Ma, J., He, H., 2012a. Influence of combustion conditions on hydrophilic properties and microstructure of flame soot. *J. Phys. Chem. A* 116, 4129–4136.
- Han, C., Liu, Y., Ma, J., He, H., 2012b. Key role of organic carbon in the sunlight-enhanced atmospheric aging of soot by O₂. *Proc. Natl. Acad. Sci. U. S. A.* 109, 21250–21255.
- Han, C., Yang, W., Wu, Q., Yang, H., Xue, X., 2016. Heterogeneous photochemical conversion of NO₂ to HONO on the humic acid surface under simulated sunlight. *Environ. Sci. Technol.* 50, 5017–5023.
- He, H., Wang, Y., Ma, Q., Ma, J., Chu, B., Ji, D., Tang, G., Liu, C., Zhang, H., Hao, J., 2014. Mineral dust and NO_x promote the conversion of SO₂ to sulfate in heavy

- pollution days. *Sci. Rep.* 4 <http://dx.doi.org/10.1038/srep04172>.
- Hung, H.-M., Hoffmann, M.R., 2015. Oxidation of gas-phase SO₂ on the surfaces of acidic microdroplets: implications for sulfate and sulfate radical anion formation in the atmospheric liquid phase. *Environ. Sci. Technol.* 49, 13768–13776.
- Jacobson, M.Z., 2001. Strong radiative heating due to the mixing state of black carbon in atmospheric aerosols. *Nature* 409, 695–697.
- Khalizov, A.F., Xue, H., Wang, L., Zheng, J., Zhang, R., 2009a. Enhanced light absorption and scattering by carbon soot aerosol internally mixed with sulfuric acid. *J. Phys. Chem. A* 113, 1066–1074.
- Khalizov, A.F., Zhang, R., Zhang, D., Xue, H., Pagels, J., McMurry, P.H., 2009b. Formation of highly hygroscopic soot aerosols upon internal mixing with sulfuric acid vapor. *J. Geophys. Res.* 114.
- Kirchner, U., Scheer, V., Vogt, R., 2000. FTIR spectroscopic investigation of the mechanism and kinetics of the heterogeneous reactions of NO₂ and HNO₃ with soot. *J. Phys. Chem. A* 104, 8908–8915.
- Kong, L.D., Zhao, X., Sun, Z.Y., Yang, Y.W., Fu, H.B., Zhang, S.C., Cheng, T.T., Yang, X., Wang, L., Chen, J.M., 2014. The effects of nitrate on the heterogeneous uptake of sulfur dioxide on hematite. *Atmos. Chem. Phys.* 14, 9451–9467.
- Lelièvre, S., Bedjanian, Y., Povesle, N., Delfau, J.-L., Vovelle, C., Le Bras, G., 2004. Heterogeneous reaction of ozone with hydrocarbon flame soot. *Phys. Chem. Chem. Phys.* 6, 1181–1191.
- Li, K., Ling, L., Lu, C., Liu, Z., Liu, L., Mochida, I., 2001. Influence of CO-evolving groups on the activity of activated carbon fiber for SO₂ removal. *Fuel Process. Technol.* 70, 151–158.
- Li, Q., Shang, J., Zhu, T., 2013. Physicochemical characteristics and toxic effects of ozone-oxidized black carbon particles. *Atmos. Environ.* 81, 68–75.
- Lin, W., Xu, X., Ge, B., Liu, X., 2011. Gaseous pollutants in Beijing urban area during the heating period 2007–2008: variability, sources, meteorological, and chemical impacts. *Atmos. Chem. Phys.* 11, 8157–8170.
- Ling, L., Li, K., Liu, L., Miyamoto, S., Korai, Y., Kawano, S., Mochida, I., 1999. Removal of SO₂ over ethylene tar pitch and cellulose based activated carbon fibers. *Carbon* 37, 499–504.
- Lisovskii, A., Semiat, R., Aharoni, C., 1997a. Adsorption of sulfur dioxide by active carbon treated by nitric acid: I. Effect of the treatment on adsorption of SO₂ and extractability of the acid formed. *Carbon* 35, 1639–1643.
- Lisovskii, A., Shter, G.E., Semiat, R., Aharoni, C., 1997b. Adsorption of sulfur dioxide by active carbon treated by nitric acid: II. Effect of preheating on the adsorption properties. *Carbon* 35, 1645–1648.
- Liu, Q., Li, C., Li, Y., 2003. SO₂ removal from flue gas by activated semi-cokes: 1. The preparation of catalysts and determination of operating conditions. *Carbon* 41, 2217–2223.
- Liu, Y., Han, C., Ma, J., Bao, X., He, H., 2015a. Influence of relative humidity on heterogeneous kinetics of NO₂ on kaolin and hematite. *Phys. Chem. Chem. Phys.* 17, 19424–19431.
- Liu, Y., Liggio, J., Li, S.-M., Breznan, D., Vincent, R., Thomson, E.M., Kumarathasan, P., Das, D., Abbatt, J., Antinolo, M., Russell, L., 2015b. Chemical and toxicological evolution of carbon nanotubes during atmospherically relevant aging processes. *Environ. Sci. Technol.* 49, 2806–2814.
- Liu, Y., Liu, C., Ma, J., Ma, Q., He, H., 2010. Structural and hygroscopic changes of soot during heterogeneous reaction with O(3). *Phys. Chem. Chem. Phys.* 12, 10896–10903.
- Lizzio, A.A., DeBarr, J.A., 1996. Effect of surface area and chemisorbed oxygen on the SO₂ adsorption capacity of activated char. *Fuel* 75, 1515–1522.
- Lizzio, A.A., DeBarr, J.A., 1997. Mechanism of SO₂ removal by carbon. *Environ. Sci. Technol.* 11, 284–291.
- Lu, P.D., Wang, F., Zhao, L.J., Li, W.X., Li, X.H., Dong, J.L., Zhang, Y.H., Lu, G.Q., 2008. Molecular events in deliquescence and efflorescence phase transitions of sodium nitrate particles studied by Fourier transform infrared attenuated total reflection spectroscopy. *J. Chem. Phys.* 129, 104509.
- Mészáros, A., Mészáros, E., 1989. Sulfate formation on elemental carbon particles. *Aerosol Sci. Technol.* 10, 337–342.
- Ma, Q., He, H., Liu, Y., 2010. In situ DRIFTS study of hygroscopic behavior of mineral aerosol. *J. Environ. Sci.* 22, 555–560.
- McCabe, J., Abbatt, J.P.D., 2009. Heterogeneous loss of gas-phase ozone on n-hexane soot surfaces: similar kinetics to loss on other chemically unsaturated solid surfaces. *J. Phys. Chem. C* 113, 2120–2127.
- Mochida, I., Kuroda, K., Miyamoto, S., Sotowa, C., Korai, Y., Kawano, S., Sakanishi, K., Yasutake, A., Yoshikawa, M., 1997. Remarkable catalytic activity of calcined pitch based activated carbon fiber for oxidative removal of SO₂ as aqueous H₂SO₄. *Environ. Sci. Technol.* 11, 272–276.
- Monge, M.E., D'Anna, B., Mazzi, L., Giroir-Fendler, A., Ammann, M., Donaldson, D.J., George, C., 2010. Light changes the atmospheric reactivity of soot. *Proc. Natl. Acad. Sci. U. S. A.* 107, 6605–6609.
- Mudunkotuwa, I.A., Minshid, A.A., Grassian, V.H., 2014. ATR-FTIR spectroscopy as a tool to probe surface adsorption on nanoparticles at the liquid-solid interface in environmentally and biologically relevant media. *Analyst* 139, 870–881.
- Ndour, M., Nicolas, M., D'Anna, B., Ka, O., George, C., 2009. Photoreactivity of NO₂ on mineral dusts originating from different locations of the Sahara desert. *Phys. Chem. Chem. Phys.* 11, 1312–1319.
- Novakov, T., Chang, S.G., Harker, A.B., 1974. Sulfates as pollution particulates catalytic formation on carbon (soot) particles. *Science* 186, 259–261.
- Pósfai, M., Anderson, J.R., Buseck, P.R., Sievering, H., 1999. Soot and sulfate aerosol particles in the remote marine troposphere. *J. Geophys. Res.* 104, 21685–21693.
- Pagels, J., Khalizov, A.F., McMurry, P.H., Zhang, R.Y., 2009. Processing of soot by controlled sulphuric acid and water condensation—mass and mobility relationship. *Aerosol Sci. Technol.* 43, 629–640.
- Peebles, B.C., Dutta, P.K., Waldman, W.J., Villamena, F.A., Nash, K., Severance, M., Nagy, A., 2011. Physicochemical and toxicological properties of commercial carbon blacks modified by reaction with ozone. *Environ. Sci. Technol.* 45, 10668–10675.
- Peng, J., Hu, M., Guo, S., Du, Z., Zheng, J., Shang, D., Zamorab, M.L., Zeng, L., Shao, M., Wu, Y.-S., Zheng, J., Wang, Y., Glen, C.R., Collins, D.R., Molina, M.J., Zhang, R., 2016. Markedly enhanced absorption and direct radiative forcing of black carbon under polluted urban environments. *Proc. Natl. Acad. Sci. U. S. A.* 113, 4266–4271.
- Penner, J.E., Eddleman, H., Novakov, T., 1993. Towards the development of a global inventory for black carbon emissions. *Atmos. Environ. Part A* 27, 1277–1295.
- Querry, M.R., Waring, R.C., Holland, W.E., Earls, L.M., Herrman, M.D., Nijm, W.P., Hale, G.M., 1974. Optical constants in the infrared for K₂SO₄, NH₄H₂PO₄, and H₂SO₄ in water. *J. Opt. Soc. Am.* 64, 39–46.
- Rubio, B., Izquierdo, M.T., 1998. Low cost adsorbents for low temperature cleaning of flue gases. *Fuel* 77, 631–637.
- Saathoff, H., Naumann, K.H., Riemer, N., Kamm, S., Möhler, O., Schurath, U., Vogel, H., Vogel, B., 2001. The loss of NO₂, HNO₃, NO₃/N₂O₅, and HO₂/HOONO₂ on soot aerosol: a chamber and modeling study. *Geophys. Res. Lett.* 28, 1957–1960.
- Saathoff, H., Naumann, K.H., Schnaiter, M., Schöck, W., Möhler, O., Schurath, U., Weingartner, E., Gysel, M., Baltensperger, U., 2003. Coating of soot and (NH₄)₂SO₄ particles by ozonolysis products of α -pinene. *J. Aerosol Sci.* 34, 1297–1321.
- Seinfeld, J.H., Pandis, S.N., 1998. *Atmospheric Chemistry and Physics from Air Pollution to Climate Change*. John Wiley and Sons.
- Smith, D.M., Chughtai, A.R., 1995. The surface structure and reactivity of black carbon. *Colloids Surfaces A Physicochem. Eng. Aspects* 105, 47–77.
- Smith, D.M., Keifer, J.R., Novicky, M., Chughtai, A.R., 1989. An FT-IR study of the effect of simulated solar radiation and various particulates on the oxidation of SO₂. *Appl. Spectrosc.* 43, 103–107.
- Sun, F., Gao, J., Zhu, Y., Chen, G., Wu, S., Qin, Y., 2013. Adsorption of SO₂ by typical carbonaceous material: a comparative study of carbon nanotubes and activated carbons. *Adsorption* 19, 959–966.
- Sun, Y., Chen, C., Zhang, Y., Xu, W., Zhou, L., Cheng, X., Zheng, H., Ji, D., Li, J., Tang, X., Fu, P., Wang, Z., 2016. Rapid formation and evolution of an extreme haze episode in Northern China during winter 2015. *Sci. Rep.* 6 <http://dx.doi.org/10.1038/srep27151>.
- Sydbom, A., Blomberg, A., Parnia, S., Stenfors, N., Sandstrom, T., Dahlen, S.E., 2001. Health effects of diesel exhaust emissions. *Eur. Respir. J.* 17, 733–746.
- Ueda, S., Nakayama, T., Taketani, F., Adachi, K., Matsuki, A., Iwamoto, Y., Sadanaga, Y., Matsumi, Y., 2015. Light absorption and morphological properties of soot-containing aerosols observed at an East Asian outflow site, Noto Peninsula, Japan. *Atmos. Chem. Phys. Discuss.* 15, 25089–25138.
- Ullerstam, M., Vogt, R., Langer, S., Ljungström, E., 2002. The kinetics and mechanism of SO₂ oxidation by O₃ on mineral dust. *Phys. Chem. Chem. Phys.* 4, 4694–4699.
- Wang, G., Zhang, R., Gomez, M.E., Yang, L., Levy Zamora, M., Hu, M., Lin, Y., Peng, J., Guo, S., Meng, J., Li, J., Cheng, C., Hu, T., Ren, Y., Wang, Y., Gao, J., Cao, J., An, Z., Zhou, W., Li, G., Wang, J., Tian, P., Marrero-Ortiz, W., Secret, J., Du, Z., Zheng, J., Shang, D., Zeng, L., Shao, M., Wang, W., Huang, Y., Wang, Y., Zhu, Y., Li, Y., Hu, J., Pan, B., Cai, L., Cheng, Y., Ji, Y., Zhang, F., Rosenfeld, D., Liss, P.S., Duce, R.A., Kolb, C.E., Molina, M.J., 2016. Persistent sulfate formation from London fog to chinese haze. *Proc. Natl. Acad. Sci. U. S. A.* 113, 13630–13635.
- Wang, Y., Khalizov, A., Levy, M., Zhang, R., 2013. New Directions: light absorbing aerosols and their atmospheric impacts. *Atmos. Environ.* 81, 713–715.
- Yamamoto, K., Seki, M., Kawazoe, K., 1972. Absorption of sulfur dioxide on activated carbon in the flue gas desulfurization process. II. Rate of oxidation of sulfur dioxide on activated carbon surfaces. *Nippon Kagaku Kaishi* 6, 1046–1052.
- Zawadzki, J., 1978. IR spectroscopy studies of oxygen surface compounds on carbon. *Carbon* 16, 491–497.
- Zawadzki, J., 1987a. Infrared studies of SO₂ on carbons—I. Interaction of SO₂ with carbon films. *Carbon* 25, 431–436.
- Zawadzki, J., 1987b. Infrared studies of SO₂ on carbons—II. the SO₂ species adsorbed on carbon films. *Carbon* 25, 495–502.
- Zhang, D., Zhang, R., 2005. Laboratory investigation of heterogeneous interaction of sulfuric acid with soot. *Environ. Sci. Technol.* 39, 5722–5728.
- Zhang, G., Bi, X., He, J., Chen, D., Chan, L.Y., Xie, G., Wang, X., Sheng, G., Fu, J., Zhou, Z., 2014. Variation of secondary coatings associated with elemental carbon by single particle analysis. *Atmos. Environ.* 92, 162–170.
- Zhang, P., Wanko, H., Ulrich, J., 2007. Adsorption of SO₂ on activated carbon for low gas concentrations. *Chem. Eng. Technol.* 30, 635–641.
- Zhang, R., Khalizov, A.F., Pagels, J., Zhang, D., Xue, H., McMurry, P.H., 2008. Variability in morphology, hygroscopicity, and optical properties of soot aerosols during atmospheric processing. *Proc. Natl. Acad. Sci. U. S. A.* 105, 10291–10296.
- Zhang, R., Wang, G., Guo, S., Zamora, M.L., Ying, Q., Lin, Y., Wang, W., Hu, M., Wang, Y., 2015a. Formation of urban fine particulate matter. *Chem. Rev.* 115, 3803–3855.
- Zhang, X.Y., Wang, J.Z., Wang, Y.Q., Liu, H.L., Sun, J.Y., Zhang, Y.M., 2015b. Changes in chemical components of aerosol particles in different haze regions in China from 2006 to 2013 and contribution of meteorological factors. *Atmos. Chem. Phys.* 15, 12935–12952.
- Zhao, Y., Ma, Q., Liu, Y., He, H., 2016. Influence of sulfur in fuel on the properties of diffusion flame soot. *Atmos. Environ.* 142, 383–392.
- Zheng, B., Zhang, Q., Zhang, Y., He, K.B., Wang, K., Zheng, G.J., Duan, F.K., Ma, Y.L., Kimoto, T., 2015a. Heterogeneous chemistry: a mechanism missing in current

models to explain secondary inorganic aerosol formation during the January 2013 haze episode in North China. *Atmos. Chem. Phys.* 15, 2031–2049.

Zheng, G.J., Duan, F.K., Su, H., Ma, Y.L., Cheng, Y., Zheng, B., Zhang, Q., Huang, T.,

Kimoto, T., Chang, D., Pöschl, U., Cheng, Y.F., He, K.B., 2015b. Exploring the severe winter haze in Beijing: the impact of synoptic weather, regional transport and heterogeneous reactions. *Atmos. Chem. Phys.* 15, 2969–2983.